

# New fast method for determination of number of UHMWPE wear particles

M. ŠLOUF<sup>1,\*</sup>, I. ŠLOUFOVÁ<sup>1</sup>, Z. HORÁK<sup>1</sup>, P. ŠTĚPÁNEK<sup>1</sup>, G. ENTLICHER<sup>2</sup>,  
M. KREJČÍK<sup>3</sup>, T. RADONSKÝ<sup>4</sup>, D. POKORNÝ<sup>4</sup>, A. SOSNA<sup>4</sup>

<sup>1</sup>*Institute of Macromolecular Chemistry of the Academy of Science of the Czech Republic, Heyrovsky Sq. 2, 16206 Prague 6, Czech Republic*

*E-mail: slouf@imc.cas.cz*

<sup>2</sup>*Department of Biochemistry, Charles University, Hlavova 2030, 12840 Prague 2, Czech Republic*

<sup>3</sup>*EKOL Ltd., M. Majerove 1152, 58401 Ledec nad Sazavou, Czech Republic*

<sup>4</sup>*Orthopaedics Clinic, Hospital Motol, V uvalu 84, 15606 Prague 6, Czech Republic*

Ultra-high molecular weight polyethylene (UHMWPE) wear particles are the major cause of total joint replacement (TJR) failures because the wear particles, released from TJR's, cause bone loosening. To simplify the study of the relationship between numbers of particles at various locations around TJR's and extent of bone loosening at these locations, the authors of this work tried to develop a new method for easy and fast determination of number of wear particles. The method, called LSC (Light Scattering with Calibration spheres), is based on light scattering of a suspension of wear particles *and* calibration spheres, and yields *relative* numbers of particles. A modified LSC method, called LSCm, requires *one* additional experiment, a gravimetric analysis of a mixture of all studied samples, to determine *absolute* numbers of wear particles. LSC and LSCm methods are easy and fast, which make them suitable for processing and comparing high number of samples.

© 2004 Kluwer Academic Publishers

## 1. Introduction

Ultra-high molecular weight polyethylene (UHMWPE) has been widely used as a bearing material in total joint replacements (TJR) for more than three decades. In spite of this fact, the bearing is still viewed as replacement's weakest point, and therefore its life-limiting factor. As generally accepted, this is due to UHMWPE wear particles originating in articulation of a bearing with associated metal or ceramic components [1–6]. Some of the wear particles are absorbed by macrophages, which launches a complex inflammatory process leading to the loss of the bone tissue in surroundings of the implant and, consequently, to its loosening. The mentioned process is usually classified in the literature as polyethylene disease and pathological tissue formed as osteoaggressive granuloma.

According to the available literature, there is almost no information on the relationship between the number of particles in particular locations in the surroundings of TJR and the extent of the bone loosening in those locations. The systematic study of the topology of UHMWPE wear particles around the TJR would help to clarify the process of osteolysis and, as a result, it might contribute to general improvement in the field

of arthroplasty. Such a study would require determining the number of wear particles from many locations around the TJR (Fig. 1) of at least tens of patients. Thus, besides the precise and verified techniques of the sampling of granuloma tissue and particle isolation, a fast and reliable method of determining the number of UHMWPE wear particles in hundreds of samples is needed. In the literature, several techniques for quantitative analysis of UHMWPE wear particles have been described. Margevicius *et al.* [7] and Maloney *et al.* [8] used electric resistance particle-size analyzer. This device determines the number and size of particles suspended in an electrolyte by monitoring the electric current between two electrodes immersed in the electrolyte on either side of a small aperture through which a suspension of particles is forced to flow. However, the lower limit of detection lies quite high, allowing calculation of only the particles with equivalent diameter higher than 0.58  $\mu\text{m}$ , while the biologically active particles can be smaller than 0.2  $\mu\text{m}$ . Tipper *et al.* [9] described the method based on weighting the wear particles and estimating their number from image analysis of micrographs of the particles on the filter. On one hand, the method is assumed to catch all particles and to be precise; on the other hand, it necessitates

\*Author to whom all correspondence should be addressed.



Figure 1 Zones (locations) around total hip replacement, from which the tissue samples were taken. The numbering of locations is similar to that used by Gruen [16] and De Lee [17]. Location "X" corresponds to periprosthetic tissue around the neck of femoral component, location "0", which is not shown in the figure, denotes unspecified location far away from TJR.

laborious and time-consuming quantitative isolation of the wear particles and requires weighable amount of particles. Scott *et al.* [10] estimated the number of particles directly, from the scanning electron micrographs of particles on filter membrane. This technique skips the determination of the particle weight at the cost of accuracy. The most common technique for *in vivo* studies of wear is radiographic method [11], in which the overall wear is determined from the differences between the initial and final RTG images. Precision of this method is rather limited and, moreover, it yields just one overall number characterizing the total wear. Weight loss method is widely used in the orthopedic device analysis [12]. It uses weight differences to describe polymeric material lost through wear. The weight loss method provides just one overall number as the previous technique and is unusable for *in vivo* studies as it relies on weighing the whole polymeric part of the joint.

As none of the above mentioned techniques was found fast and/or precise enough, the authors of this work tried to develop a new method for determination of the number of UHMWPE wear particles. The new method is denoted as LSC (Light Scattering with Calibration) and is based on the scattering of light by a dispersion of wear particles and calibration spheres. The LSC method is quite fast because it requires just a simple isolation technique for wear particles. The method is also relatively straightforward as its key step is a routine LS experiment. These features make it suitable for processing high numbers of samples. The description of LSC method and the first results are given in this work. The application of the LSC method for systematic study of the topology of UHMWPE wear particles

around TJR will be described elsewhere [13]. In the course of work the authors found that a similar method is used in cytometry [14]. Moreover, some recent particle counters, whose principle is light scattering, are able to determine the numbers of wear particles directly [15].

## 2. Experimental

### 2.1. Sampling

Seventy-three samples of periprosthetic granulomatous membranes were harvested in 18 patients who underwent TJR revision surgery for aseptic loosening. Tissue samples were retrieved from 3 acetabular (zones 8, 9, 10) and 7 femoral locations (zones 1 to 7) according to the topographic scheme that was based on radiological zoning of periprosthetic osteolysis as described by DeLee [16] and Gruen [17]. We slightly modified this scheme by adding zone "X" that corresponds with the periprosthetic tissue located around the neck of the femoral component and zone "0" that denotes a sample taken from unspecified location far away from TJR (Fig. 1). Retrieved samples were stored in special containers under standard conditions (dark and dry place, 3–5 °C) prior to further processing. Maximum time before processing was 72 h. In the following text, the samples are denoted as X/Y, where X is the patient number and Y is the location number.

### 2.2. Isolation of UHMWPE wear particles

#### 2.2.1. Isolation I

The key method of this work was light scattering from the suspensions containing UHMWPE particles. The suspensions for LS were prepared by digestion of samples with nitric acid. HNO<sub>3</sub> digestion was used because of its simplicity and easy application to relatively large amounts of granuloma. Fresh samples of granuloma (0.2–6.5 g) were freeze-dried and UHMWPE particles were isolated from the freeze-dried samples of granuloma essentially as described by Margevicius *et al.* [7]. However, much larger samples were used for isolation to obtain more reliable results. All samples were hydrolyzed with appropriate amount of HNO<sub>3</sub>; Typically 10 ml of concentrated HNO<sub>3</sub> pre-filtered with 0.4 μm filter (Synpor) was used for 0.3 g of freeze-dried sample. After 24 h of incubation of the sample in HNO<sub>3</sub> at laboratory temperature the suspension was mixed with a minishaker for 2 min and again incubated for 24 h at laboratory temperature. The solution was then centrifuged at 16 400 g for 20 min. Most of the solution between the floating and sedimenting particles was carefully aspirated and discarded. The residue was washed twice with 5 ml of concentrated HNO<sub>3</sub> and once with 5 ml of pre-filtered distilled water (0.4 μm filter, Synpor) under the same conditions of centrifugation and aspiration of the solution between sedimenting and floating particles. The final residue was suspended in 8 ml of pre-filtered distilled water; pH was adjusted to 7.5–8.0 with 2 mol/l NaOH and diluted to 10 ml with

pre-filtered distilled water. Then the samples were kept at  $-16^{\circ}\text{C}$ .

### 2.2.2. Isolation II

Several samples were analyzed by other methods than light scattering to verify the results. If the methods required removal of soluble impurities, such as nitrate salts from the  $\text{HNO}_3$  digestion, the dialysis was employed. The samples were prepared as described in Section 2.2.1 and dialyzed against  $3 \times 10$  l of distilled water for 72 h at  $4^{\circ}\text{C}$ . Regular dialysis tubings (Sigma) for protein dialysis were used.

### 2.2.3. Isolation III

Isolation III is a quantitative isolation of UHMWPE particles. The LSC method gives relative numbers of UHMWPE particles. If the absolute numbers of UHMWPE particles are needed, combining all samples, carrying out isolation III and some additional calculations are necessary. Quantitative isolation of UHMWPE particles was performed as follows: the rests of the samples that were used for light scattering were all combined and centrifuged at  $16\,400\text{ g}$  for 20 min. The supernatant was collected and filtered with a  $5\text{-}\mu\text{m}$  filter (Sartorius). The pore size of  $5\text{ }\mu\text{m}$  was selected because it had been proved that the number of bigger particles is negligible [7–10, 18, 19]. The filtrate was ultracentrifuged at  $250\,000\text{ g}$  and the supernatant filtered with a pre-weighed and pre-washed ultrafiltration membrane PM 30 (Amicon). The residue on the membrane was washed three times with ultrafiltered distilled water. The membrane was then dried and weighed. The weight difference was compared with that of control membranes. The resulting total weight of the particles was used as an absolute value enabling quantitative interpretation of light scattering results as described in Section 3.3.

### 2.3. Light microscopy

Light microscope (Zetopan Pol, Reichert) equipped with polarizers, heating stage FP52/FP5 (Mettler) and digital camera (Cohu) was used to identify UHMWPE particles in the samples. A sample, prepared as described in Section 2.2.2, was observed in both transmission and polarized light while the temperature was increased ( $2^{\circ}\text{C}/\text{min}$ ). At low temperatures, the UHMWPE particles appear bright in polarized light because the UHMWPE is a semicrystalline polymer exhibiting birefringence [20]. At UHMWPE melting temperature ( $T_m \approx 110\text{--}140^{\circ}\text{C}$  [20]), crystallinity and birefringence are vanishing and the UHMWPE particles turn black.

### 2.4. Infrared microscopy

Infrared (IR) spectra were measured with Fourier transform infrared (FTIR) spectrometer (Magna-IR 760, Nicolet E.S.P.) equipped with infrared microscope using attenuated total reflection (ATR) single reflection method (ZnSe crystal,  $675\text{--}4000\text{ cm}^{-1}$  region,  $4\text{ cm}^{-1}$  resolution, 256 scans, triangular apodization). Samples

prepared as described in Section 2.2.1 and Section 2.2.2 were used for the IR analysis.

### 2.5. Differential scanning calorimetry

DSC measurements were made on Perkin Elmer DSC Pyris 1. The temperature and power scales of the calorimeter were calibrated using indium and sapphire as standards. The measurement was carried in helium atmosphere with liquid nitrogen as coolant. Heating and cooling rates  $20\text{ K}/\text{min}$  were used. Approx.  $10\text{ mg}$  of the sample (prepared by the technique described in Section 2.2.1) was placed into sealed pan and used for the measurement in the standard DSC mode.

### 2.6. Elastic light scattering

The suspensions of UHMWPE particles were analyzed using Coulter LS 230. The instrument uses either Fraunhofer or Mie theory [21–23] to predict volume distribution of the particles in suspension from scattering of laser light. LS 230 measures particles from  $0.04\text{ }\mu\text{m}$  to  $2000\text{ }\mu\text{m}$ . At the beginning of the measurement, the analyzed particles are added to  $150\text{ ml}$  of circulating medium until a suitable concentration of the particles is achieved, which is indicated by the controlling software. As for the samples, the suspension of UHMWPE particles, prepared as described in Section 2.2.1, was added to the circulating liquid, until the minimum suitable concentration was achieved and the first set of scattering data was collected. In the next step, a weighed amount of glass calibration spheres was added to the circulating medium so that the maximum suitable concentration was not exceeded and second scattering data set was collected. From the two sets of the data it is possible to extract information about the number of the measured particles as described below in Sections 3.2 and 3.3. The scattering was measured for  $90\text{ s}$  to ensure sufficient signal. The circulating medium was water with added non-identified surfactant (Simple Green, USA) to prevent agglomeration. The optical model was:  $n_{\text{real}}(\text{sample}) = 1.55$ ,  $n_{\text{imag}}(\text{sample}) = 0.1$  and  $n_{\text{real}}(\text{medium}) = 1.33$ , where  $n_{\text{real}}$  is the real part of refractive index,  $n_{\text{imag}}$  is the imaginary parts of refractive index, sample is UHMWPE and medium is water. Mie theory was used to calculate volume distributions because the usage of simplified Fraunhofer theory for particles smaller than  $10\text{ }\mu\text{m}$  is not recommended. PIDS (Polarization Intensity Differential Scattering) assembly of Coulter LS 230 was used to obtain information about the particles smaller than  $0.4\text{ }\mu\text{m}$ . The PIDS assembly uses beams of light with three different wavelengths polarized both vertically and horizontally and measures the differences in scattered intensities among these beams. As a result, it enhances resolution and provides size information for particles from  $0.04\text{ }\mu\text{m}$  to  $0.4\text{ }\mu\text{m}$ .

### 2.7. X-ray diffraction

Diffraction patterns were obtained with four-circle diffractometer Nonius KappaCCD (Nonius;  $\text{Mo K}\alpha$  radiation,  $\lambda = 0.71\text{ \AA}$ , two-dimensional CCD detector

with diameter 9.1 cm). The powder-like diffraction patterns were obtained by a single rotation scan. The experimentally obtained powder diffraction patterns were compared with those theoretically calculated. The calculation was performed with program LAZY PULVERIX [24]. The crystallographic data for the calculation were taken from ICSD [25].

## 2.8. Quasi-elastic light scattering

The quasi-elastic light scattering (QELS) instrument employed an ALV5000/E correlator. The light source was a HeNe laser Hewlett-Packard 125A with wavelength 632 nm. Temperature was controlled ( $\pm 0.1$  °C) with a Lakeshore 330 temperature controller. The correlator was operated in the crosscorrelation mode, which ensures that all artifacts due to after-pulsing and other imperfections do not affect the correlation function in the early time regime. The measured intensity correlation functions  $g^2(t)$  were analyzed using nonlinear inverse Laplace transformation to obtain the distributions of relaxation times  $A(\tau)$  using the equation  $g^2(t) - 1 = \alpha [\int \tau A(\tau) \exp(-t/\tau) d\tau]^2$ , where  $\alpha$  is an instrumental parameter. The obtained relaxation times  $\tau$  were converted into diffusion coefficients  $D$  using the standard relation  $D = (\tau q^2)^{-1}$  and hydrodynamic radii  $R_H$  were calculated from  $D$  using the Stokes-Einstein relation  $D = (kT)/(6\pi\eta R_H)$ , where  $k$  is the Boltzmann constant,  $T$  is the absolute temperature and  $\eta$  is the viscosity of the solvent. The samples for QELS measurements were filtered through a 0.8  $\mu\text{m}$  Millipore filter into dedusted light scattering cells and thermostatted at 25 °C.

## 2.9. Scanning electron microscopy

A drop of suspension of UHMWPE particles prepared as described in Section 2.2.2 (isolation II) was placed on a smooth surface of mica and left to evaporate at room temperature. The mica with the dry particles was covered with a thin platinum film to avoid charging during the electron-microscope observation. The samples were observed with scanning electron microscope (SEM) Jeol JSM 6400 using secondary electrons.

## 2.10. Energy dispersive X-ray analysis

A drop of suspension of UHMWPE particles prepared as described in Section 2.2.2 (isolation II) was placed on a carbon block (cylinder, 5 mm in diameter, 3 mm high) and left to evaporate at room temperature. Then the samples were covered with a thin carbon film to avoid charging in the electron microscope. The energy dispersive X-ray analysis (EDAX) was performed using JEOL SUPERPROBE 733 scanning electron microscope equipped with JXA 733 X-ray analyzer and KEVEX  $\Delta$  EDX spectrometer.

## 3. Results

### 3.1. Isolation and preliminary characterization of UHMWPE particles

The first part of this study comprised: (1) sampling, (2) extraction of UHMWPE particles from the samples and

(3) preliminary characterization of the extracted particles. The sampling and the extraction of the UHMWPE particles have been described in the experimental section above. As for the characterization of extracted particles, four methods were used: polarized-light microscopy, FTIR microscopy, DSC and XRD. The goal was to prove that the samples do contain UHMWPE particles, to find possible impurities and to modify extraction procedure if the amount of impurities was too high.

Visual inspection of the samples indicated that some samples contain insoluble impurities. The impurities did not float but were located at the bottom of the flasks, which implies that their density was higher than 1 g/cm<sup>3</sup>. The polarized-light microscopy showed that samples contained the particles that were birefringent up to approx. 120 °C, which corresponds to the melting temperature of PE [20]. The observed UHMWPE particles ranged from 1 to 20  $\mu\text{m}$  in size and were mostly flat and round in shape. The submicron particles could not be observed because of the limited resolution of the optical microscope. In addition, there were also some non-birefringent particles in the samples. They might have been impurities of organic origin; hence the extraction procedure was modified so that their number was minimized. In FTIR microscopy spectra of the samples (Fig. 2), typical polyethylene bands were detected: C–H stretching at 2916 cm<sup>-1</sup> and 2846 cm<sup>-1</sup>, CH<sub>2</sub> bending at 1471 cm<sup>-1</sup> and 1462 cm<sup>-1</sup> and CH<sub>2</sub> rocking at 729 cm<sup>-1</sup> and 718 cm<sup>-1</sup>. Differential scanning calorimetry (DSC) measurements were employed to prove that samples after the HNO<sub>3</sub> digestion do contain UHMWPE and do not contain PMMA, which is used as cement in total joint replacements. On DSC curve, a big peak corresponding to UHMWPE, several small peaks corresponding probably to some impurities but no peak of PMMA were observed. The XRD was used to analyze an unusually big particle (diameter approx. 0.5 mm), which was found in one of the samples. The particle was fixed to a thin glass fiber with epoxy glue, the fiber

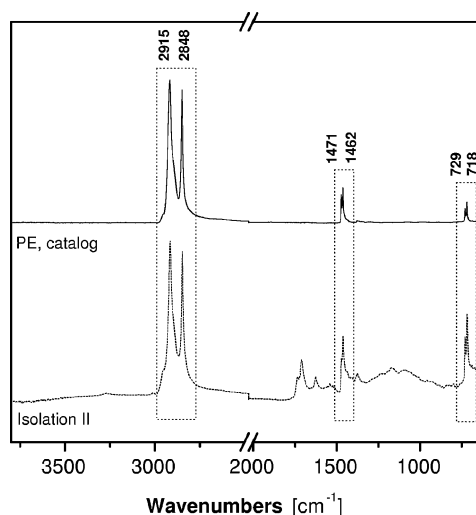


Figure 2 Infrared spectra of pure polyethylene taken from catalog and infrared spectra of UHMWPE wear particles suspension after isolation II (Chapter 2.2.2).

was fastened to the goniometer head and a diffraction pattern was recorded with a four-circle diffractometer. The diffraction pattern was found to be almost identical with the calculated powder diffraction pattern of hydroxylapatite  $\text{Ca}_{10}(\text{PO}_4)_6(\text{OH})_2$ . Moreover, in the FTIR spectrum of the particle bands corresponding to  $\text{PO}_4^-$  were observed. This suggests that the particle was a fragment of bone as the hydroxylapatite is an important component of the human bones. This assumption was further confirmed by EDAX as discussed in Section 3.4.

To conclude, the methods used for the preliminary characterization of the extracted wear debris showed that the samples contained mostly the UHMWPE particles and, in some cases, also small amount of impurities. Soluble impurities, such as nitrates and unidentified organic compounds, were unimportant, as they are unobservable by light scattering, which was used for quantitative analysis of wear debris. Insoluble organic impurities were observed in a few samples. XRD study suggested that at least some of them were small parts of bones. The insoluble impurities could have been a source of error, although their number was probably quite small as documented by IR spectra (Fig. 2). Further improvement of the extraction procedure would be helpful in this case.

### 3.2. Determination of relative numbers of UHMWPE particles

In the second and key part of this work, relative numbers of UHMWPE wear particles were determined by means of elastic light scattering (LS, Section 2.6). In principle, a standard LS experiment yields only the information on size distribution, the information on the numbers of particles is lost. That is why the authors of this work developed, tested and used a slightly modified LS method called LSC, which consists in measurement of LS of the suspension of *both* wear particles *and* a known amount of calibration spheres. The principle of the LSC method is shown in Fig. 3. At the very beginning, the samples are digested with nitric acid as described in Section 2.2.1. After this procedure, each sample is a suspension of UHMWPE particles of volume  $V_{\text{all}}$ . Each sample contains wear particles coming from a dry tissue of a known weight  $m_{\text{tissue}}$ .

In the first step of LSC method, a part of each sample (volume  $V_{\text{measured}}$  of the total volume  $V_{\text{all}}$ ) is taken, LS of the suspension of wear particles is measured and the volume distribution curves (Fig. 3(a)) are obtained. The volume distributions curves show, primarily, peaks corresponding to particles with  $d > 10 \mu\text{m}$  ( $d$  = equivalent diameter of the particle) although it is well known from the literature [7–10, 18, 19] that most of the UHMWPE wear particles have size less than  $1 \mu\text{m}$ . This is caused by the fact that that volume is proportional to  $d^3$  and so the small particles are almost negligible as far as the volume is concerned. Nevertheless, the volume distributions can easily be converted to number distributions by dividing each point of the volume distribution curve by  $d^3$ . After the conversion, the situation is just the reverse: the peaks corresponding to low numbers of big particles are negligible and peaks corresponding to high

numbers of small particles dominate the distribution curves (ref. [26], Fig. 3(e)).

In the second step of the LSC method, glass calibration spheres (of known weight  $m_{\text{spheres}}$ ) are added to each sample, LS of the mixed suspension is measured and somewhat changed volume distributions (Fig. 3(b)) result. The calibration spheres must have different size than the studied particles. In this study, the glass calibration spheres had diameter approx.  $500 \mu\text{m}$ , which accords with the peak at  $541 \mu\text{m}$  observed for each sample (Fig. 3(b)). As a known amount of calibration spheres has been added, a piece of quantitative information has been introduced in LS experiment, which can be employed in determining the relative numbers of wear particles as described below.

The first two steps of the LSC method are experimental while all the next steps include only calculations.<sup>1</sup>In the third step it is necessary to perform several numerical corrections, such as background correction, corrections for equal values of  $V_{\text{all}}$ ,  $V_{\text{measured}}$ ,  $m_{\text{spheres}}$ ,  $m_{\text{tissue}}$  and scaling. For future discussions it is convenient to divide volume distribution curves into two regions: (a) UHMWPE wear particles region ranging from the beginning of the curve at  $0.04 \mu\text{m}$  to  $300 \mu\text{m}$  and (b) glass calibration spheres region from  $300 \mu\text{m}$  to the end of the curve at  $2000 \mu\text{m}$ , with a peak at  $514 \mu\text{m}$ . The background correction is applied in the calibration spheres region. The correction is necessary because it may happen that some UHMWPE particles interfere in the calibration spheres region and form undesirable background, which has to be subtracted in a usual way. The correction may be schematically written as:

$$V_b = V\% - \text{background\_due\_to\_UHMWPE\_particles}, \quad (1)$$

where  $V_b$  are points of the volume distribution curve in calibration spheres region corrected for the background and  $V\%$  are corresponding points on volume distribution curve. Equation 1 means: for each point of the distribution curve in the calibration spheres region subtract the background due to UHMWPE particles (Fig. 3(c)). The correction for  $m_{\text{spheres}}$  is also applied in the calibration spheres region. The values of  $m_{\text{spheres}}$  for each sample may be different and the purpose of the correction is to relate all curves to the unit mass of calibration spheres. That is why the points on the volume distribution curve in the calibration spheres region have to be divided by the value of  $m_{\text{spheres}}$ :

$$V_{\text{bm}} = V_b / m_{\text{spheres}}, \quad (2)$$

where  $V_{\text{bm}}$  are points of volume distribution curve in the calibration spheres region after background correction and correction for  $m_{\text{spheres}}$ . Equation 2 means: divide each point of  $V_b$  curve in the calibration spheres region by the value of  $m_{\text{spheres}}$ . The correction for  $V_{\text{all}}$

<sup>1</sup>As the LSC method introduced in this work is new, there is no commercial program for automating the calculations. However, a self-calculating Microsoft Excel workbook with explanatory comments is available on request.

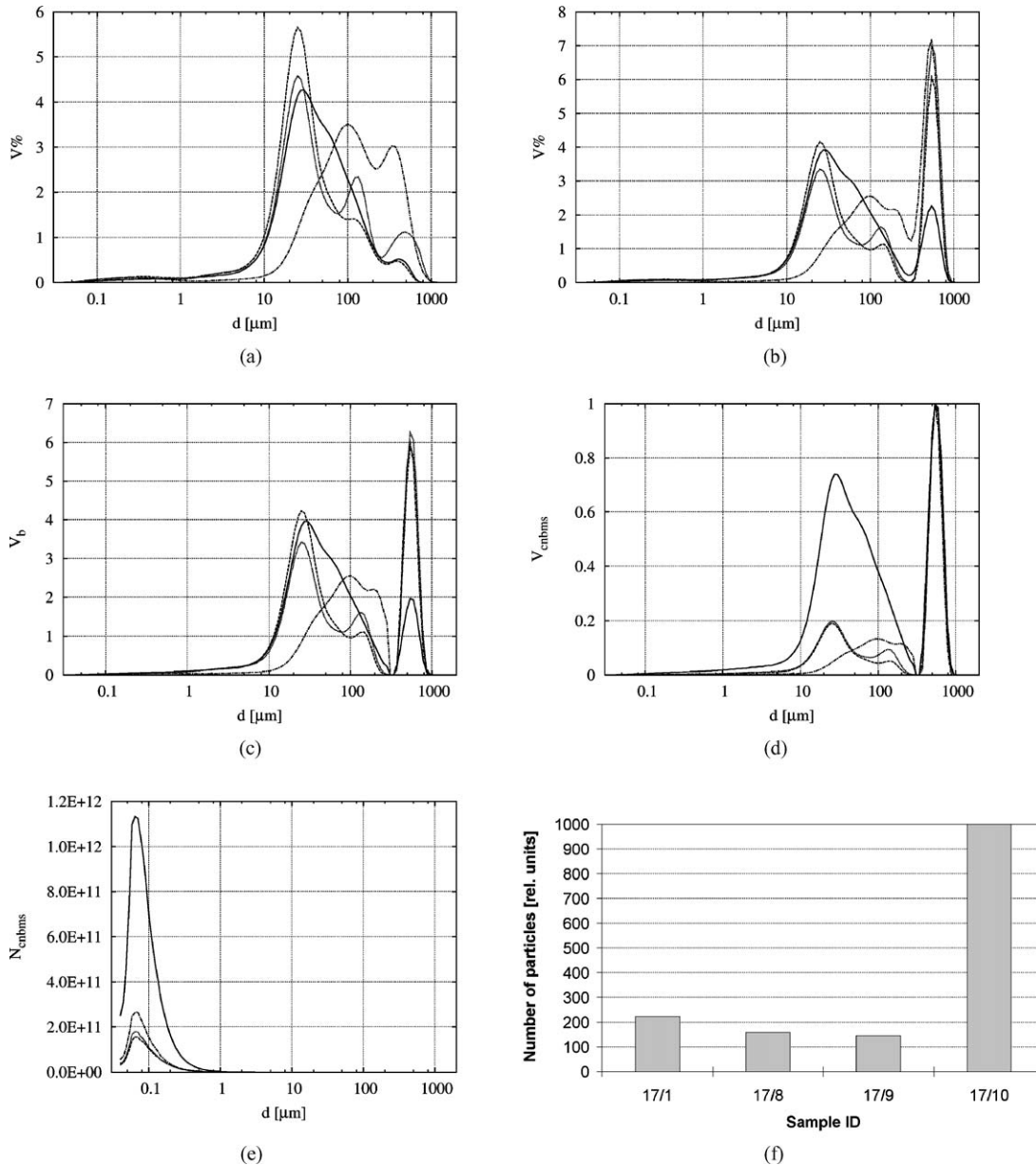


Figure 3 Determination of *relative* numbers of UHMWPE wear particles. All figures contain four LS volume distributions, corresponding to four sets of wear particles isolated from four different locations of patient 17. The locations (cf. Fig. 1) are: 1 (dotted line), 8 (dot-and-dashed line), 9 (dashed line) and 10 (full line). The figures illustrate the steps of LSC method: (a) volume distribution of suspensions of wear particles, (b) changed volume distribution of suspensions of wear particles after adding calibration spheres, (c) volume distributions after background correction in calibration spheres region, (d) volume distributions after all other corrections and normalizations, (e) number distribution curves giving relative numbers of particles and (f) final result—relative numbers of wear particles (with diameters ranging from 0.04 to 5  $\mu\text{m}$ ) in various locations for patient 17.

and  $V_{\text{measured}}$  is applied in the wear particles region. The goal of the correction is to simulate a situation as if LS from all wear particles in the sample has been measured. As it can be drawn from elementary considerations, the correction can be schematically written as:

$$V_c = V\% \times (V_{\text{all}}/V_{\text{measured}}), \quad (3)$$

where  $V_c$  are points of volume distribution curve in the UHMWPE particles region corrected for  $V_{\text{all}}$  and  $V_{\text{measured}}$ , and  $V\%$  are corresponding points on volume distribution curve. Equation 3 mean: multiply each point of  $V\%$  curve in the wear particles region with the value of  $(V_{\text{all}}/V_{\text{measured}})$ . The correction for  $m_{\text{tissue}}$  is applied in the particles region. As the values of  $m_{\text{tissue}}$

for each sample may be different, it is necessary to relate the number of UHMWPE particles to unit weight of dry tissue using the formula:

$$V_{\text{cn}} = V_c/m_{\text{tissue}}, \quad (4)$$

where  $V_{\text{cn}}$  are points on volume distribution curve after corrections for  $V_{\text{all}}$ ,  $V_{\text{measured}}$  and  $m_{\text{tissue}}$ , i.e. points representing normalized volume distribution curve, related to unit weight of dry tissue. The last correction is applied in the calibration spheres region and consists in scaling all volume distribution curves so that they could be compared with one another directly. In this study the calibration spheres are almost monodisperse, having a sharp peak at 514  $\mu\text{m}$  and so the scaling is performed by simple dividing all values of the distribution curve

in the calibration spheres region by the value found at  $514 \mu\text{m}$ :

$$V_{\text{bms}} = V_{\text{bm}} / V_{\text{bm\_value\_at\_514\_}\mu\text{m}}, \quad (5)$$

where  $V_{\text{bms}}$  are points on the volume distribution curve after background correction, correction for  $m_{\text{spheres}}$  and scaling, i.e. points representing scaled volume distribution curve, related to unit weight of added calibration spheres (Fig. 3(d)). The volume distribution curve after all corrections is obtained by combining the corrected distribution curve in the wear particles region and the corrected distribution curve in the calibration spheres region, which can be symbolically expressed as:

$$V_{\text{cnbms}} = V_{\text{cn}} \cup V_{\text{bms}}, \quad (6)$$

where  $V_{\text{cnbms}}$  are the points in the volume distribution curve after all corrections and symbol  $\cup$  means union of the two curves, which results in the final corrected volume distribution curves as shown in Fig. 3(d).

The fourth and last step of the LSC method is transformation of volume distributions to number distributions and calculation of relative numbers of wear particles from the distributions. The conversion of volume distribution curves to number distribution curves is achieved by dividing each point of the volume distribution curve by the value of the third power of equivalent diameter at that point, according to the formula:

$$N_{\text{cnbms}} = V_{\text{cnbms}} / d^3, \quad (7)$$

where  $N_{\text{cnbms}}$  are points of the number distribution curve after all corrections and  $d^3$  the third power of equivalent diameters. The number distribution curves are shown in Fig. 3(e). The curves on Fig. 3(e) have several characteristic features: (i) the peaks at high values of  $d$ , which dominated the volume distribution curves, vanished because big particles had large volume but their number was small. (ii) The area under curve (AuC) yields the *relative number* of wear particles, i.e. if, for example, the AuC for sample A were twice higher than the AuC for sample B then the sample A would contain twice higher number of wear particles. (iii) Nevertheless, the AuC does not yield *absolute numbers* of the particles. This is caused by the fact that the height and position of the peaks depend on selected optical model, which is defined by means of refractive indices of the studied particles and the medium. The optical model used in this study was suitable for UHMWPE ( $n_{\text{real}} = 1.55$ ,  $n_{\text{imag}} = 0.1$ ; Section 2.6) but not for calibration spheres, whose optical characteristics are different ( $n_{\text{real}} \approx 1.5$  but  $n_{\text{imag}} = 0$ ), and so the absolute numbers of glass calibration spheres must be wrong and, as a result, the absolute numbers of UHMWPE wear particles must be wrong as well. Moreover, it is known from the literature [27] that determination of size distributions by LS may be imprecise if the scattering particles are small in comparison with the wavelength  $\lambda$  of the scattered light. Thus, it should be assumed that the LS signal represented by  $N_{\text{bcns}}$  curve corresponding to very small wear particles might be imprecise, which

can be expressed as:

$$N_{\text{abs}}(d) = \text{Const} \times N_{\text{cnbms}}(d), \quad (8)$$

where  $N_{\text{abs}}(d)$  is the absolute number of wear particles with size  $d$ ,  $\text{Const}$  is a constant and  $N_{\text{cnbms}}(d)$  is the point of  $N_{\text{cnbms}}$  curve at value  $d$ . As the value of  $\text{Const}$  is not known, the absolute numbers of wear particles cannot be calculated. Provided that the wear particles and calibration spheres had exactly the same refractive indexes, if the wear particles were significantly bigger than the wavelength of scattered light, and if the volume of the particles would be equal to  $d^3$  without any other constants, the  $\text{Const}$  would be equal to 1. With decreasing size  $d$  of the particles the value of  $\text{Const}$  starts to change, especially if  $d$  approaches  $\lambda$ . This implies that Equation 8 would hold exactly only if the wear particles were monodisperse because  $\text{Const}$  is probably a function of  $d$  rather than a constant. However, the size distributions of UHMWPE wear particles are similar to each other and relatively narrow, which means that (i) Equation 8 can be regarded as a reasonable approximation, (ii) the value of  $\text{Const}$  is approximately the same for each sample because all samples contain more-or-less identical particles from the point of view of their size and refractive indexes, and (iii) it is possible to give up the determination of *absolute* numbers of wear particles and determine *relative* numbers of wear particles of size  $d$  using simple relation:

$$N_{\text{rel}}(d) = N_{\text{cnbms}}(d), \quad (9)$$

where  $N_{\text{rel}}(d)$  is a relative number of wear particles with size  $d$ . The AuC, which yields relative number of particles, is routinely calculated as:

$$N_{\text{rel}} = \sum_{d=\text{min}}^{\text{max}} N_{\text{rel}}(d), \quad (10)$$

where  $N_{\text{rel}}$  is the relative number of wear particles with  $d$  ranging from min to max. In this study, the values  $\text{min} = 0.04 \mu\text{m}$  and  $\text{max} = 5 \mu\text{m}$  were used. The value of min corresponds to the lower detection limit of the LS instrument and the value of max was selected to correspond with the filter pore size for the reasons given in Sections 2.2.3 and 3.3. The results are summarized in Fig. 3(f), which shows relative numbers of particles at different locations around TJR for patient 17. Vertical axis scale was relative as discussed in the previous paragraph and so it was re-scaled to the maximum value of 1000. Fig. 3(f) confirms the assumption of the authors that the distribution of wear particles around TJR's is quite irregular. Fig. 3 shows, for sake of simplicity, results for just one patient and only four locations. However, it should be emphasized here that LSC method is suitable especially for comparison of higher numbers of locations and patients because of its simplicity and quickness.

### 3.3. Determination of absolute numbers of UHMWPE particles

The information about relative numbers of wear particles should be sufficient in most cases. In this work, for instance, topology of UHMWPE wear particles around the TJR's was studied. In such a case, the information about the absolute numbers of wear particles is not needed: the differences among the amounts of wear particles from various locations and/or patients are exactly the same on both relative and absolute scale. However, the absolute numbers of UHMWPE particles are accessible as well, on condition that one more experiment is carried out and the calculations are modified slightly. The modified LSC method, which yields absolute numbers of particles, is denoted LSCm in the following text. Generally speaking, the modification consists in determination of  $Const$  from Equation 8, which enables direct calculation of absolute numbers of wear particles.

The first two steps of the LSCm method are identical with the first two steps of the LSC method: a suspension of UHMWPE particles without and with calibration spheres is measured for each sample. In fact there is no need to repeat the experiments and so the diffraction data from the LSC method are used for the LSCm method as well. The third step of the LSCm method, which includes calculations, is slightly different: background correction (Equation 1), correction for  $m_{spheres}$  (Equation 2), correction for  $V_{all}$  and  $V_{measured}$  (Equation 3) and scaling (Equation 5) are performed in the same way as in the LSC method, but the correction for  $m_{tissue}$  (Equation 4) has to be omitted at this stage. The final result of the third step is  $V_{cbms}$  curve, i.e. the volume distribution curve, which differs from the  $V_{cbms}$  distribution curve (Equation 6) only in the fact that it is *not normalized* for the unit weight of  $m_{tissue}$ .

The fourth step of the LSCm method is experimental. The additional experiment that has to be carried out is *one* gravimetric analysis for all studied samples. All the suspensions of wear particles that remained after LSC measurements are combined in one flask. All particles smaller than  $5 \mu m$  are extracted, purified, dried and weighed as described in Section 2.2.3. In the end, total mass  $m_{all}^{exp}$  is obtained, which gives the mass of all wear particles without those that have been taken for LSC measurements.

In the fifth step, a constant transforming relative numbers of the particles to absolute numbers of the particles is determined using the value of  $m_{all}^{exp}$ . At first, a relation for relative volume of wear particles is introduced by:

$$V_{rel}(d) = V_{cbms}(d), \quad (11)$$

where  $V_{rel}(d)$  is the relative volume of wear particles of size  $d$ , which is equal to the corresponding point  $V_{cbms}(d)$  on distribution curve  $V_{cbms}$ . In other words: the  $V_{cbms}$  curve gives the relative volumes of wear particles. Equation 11 is an analogy of Equation 9 and differs in two aspects only: (i) it concerns volumes, not numbers and (ii) the volumes were not normalized per unit weight of dry tissue. At second, the relative mass of

particles smaller than  $5 \mu m$  in each sample is calculated:

$$m_{rel} = \sum_{d=\min}^{\max} V_{rel}(d) \times \rho, \quad (12)$$

where  $\rho$  is the density of UHMWPE and the other parameters have already been defined above. The summation runs from  $0.04$  to  $5 \mu m$  as in Equation 10 and so  $m_{rel}$  provides the relative mass of the particles with  $d \leq 5 \mu m$ . As soon as the values of  $m_{rel}$  for each sample are available, the following expression is easily derived for  $m_{all}^{exp}$ :

$$m_{all}^{exp} = x \sum_{i=1}^N \left[ m_{rel,i} \times \left( 1 - \frac{V_{measured,i}}{V_{all,i}} \right) \right], \quad (13)$$

where  $x$  is an unknown constant and  $N$  is the number of the samples. The values of  $m_{rel}$ ,  $V_{measured}$  and  $V_{all}$  have already been defined above; the subscript  $i$  at those values means that they relate to  $i$ -th sample. As all the values of  $m_{all}^{exp}$ ,  $m_{rel,i}$ ,  $V_{measured,i}$  and  $V_{all,i}$  are known, the constant  $x$  can be calculated from Equation 11 directly. Knowing the constant  $x$ , it is possible to calculate the mass  $m_{all}^{abs}$ , which yields the number of all particles smaller than  $5 \mu m$ , including those used for the LSC method, in all samples according to the formula:

$$m_{all}^{abs} = x \sum_{i=1}^N m_{rel,i} = x \times m_{all}^{rel}, \quad (14)$$

where  $m_{all}^{rel}$  is the sum of all relative masses  $m_{rel}$  of all particles smaller than  $5 \mu m$  in all samples. Now let us assume that just one sample was used for gravimetric analysis, i.e. for the fourth step of the LSCm method. This may have been caused, for example, by the fact that all samples but one were completely used up, i.e. all the volumes  $V_{measured,i}$  in Equation 13 were equal to  $V_{all,i}$  except for just one sample  $i$ . In such case, Equation 13 would have still held and the constant  $x$  would have remained unchanged. It follows from the above and analogous considerations that:

$$m_{abs,i} = x \times m_{rel,i}, \quad (15)$$

where  $m_{abs,i}$  is the absolute mass of the wear particles smaller than  $5 \mu m$  in the  $i$ -th sample and  $m_{rel,i}$  is the relative mass of the wear particles smaller than  $5 \mu m$  in the  $i$ -th sample. Equation 15 shows that  $x$  is the constant, which transforms relative units to absolute ones. Thus the constant  $x$  from Equations 13–15 can be used as a replacement of  $Const$  from Equation 8 because the two constants do the same thing: they change relative scale to absolute scale.

In the sixth and last step of the LSCm method, constant  $x$  is used to determine absolute numbers of wear particles. This step includes only calculations that are applied in the region between the constants  $\min$  and  $\max$  as defined in Equations 10 and 12. At first, relative mass distribution curves  $m_{cbms}^{rel}$  are calculated using



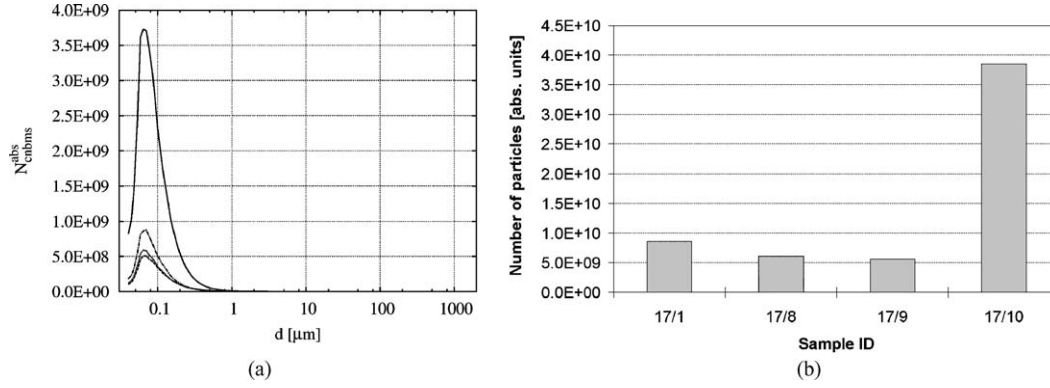


Figure 4 Determination of *absolute* numbers of UHMWPE wear particles: (a) number distribution curves giving absolute numbers of particles and (b) final result—absolute numbers of wear particles (with diameters ranging from 0.04 to 5  $\mu\text{m}$ ) in various locations for patient 17.

Equation 16 and converted to absolute mass distribution curves  $m_{\text{cbms}}^{\text{abs}}$  using Equation 17:

$$m_{\text{cbms}}^{\text{rel}} = V_{\text{cbms}} \times \rho, \quad (16)$$

$$m_{\text{cbms}}^{\text{abs}} = m_{\text{cbms}}^{\text{rel}} \times x. \quad (17)$$

Distribution curve  $m_{\text{cbms}}^{\text{abs}}$  can be recalculated to  $N_{\text{cbms}}^{\text{abs}}$  distribution curve yielding absolute numbers of wear particles, on condition that the wear particles are spheres with diameter  $d$ . This quite reasonable approximation as  $d$  is defined as a diameter of equivalent sphere in LS. The  $N_{\text{cbms}}^{\text{abs}}$  curve is given by:

$$N_{\text{cbms}}^{\text{abs}} = \frac{6m_{\text{cbms}}^{\text{abs}}}{\pi\rho \times d^3}. \quad (18)$$

Distribution curve  $N_{\text{cbms}}^{\text{abs}}$  normalized per unit weight of dry tissue is obtained by dividing each point of  $N_{\text{cbms}}^{\text{abs}}$  by  $m_{\text{tissue}}$ :

$$N_{\text{cbms}}^{\text{abs}} = N_{\text{cbms}}^{\text{abs}} / m_{\text{tissue}}; \quad (19)$$

each point of the  $N_{\text{cbms}}^{\text{abs}}$  curve gives the absolute number of wear particles of given diameter  $d$ , normalized per unit weight of dry tissue (Fig. 4(a)). The normalization has to be performed here, *after* the gravimetric analysis (the fourth step of the LSCm method) and following calculations of constant  $x$  (the fifth step of the LSCm method), because non-normalized amounts of wear particles are dealt with during the fourth step. The absolute numbers of wear particles  $N_{\text{abs}}$ , with equivalent diameters  $d$  ranging from min to max, normalized per unit weight of dry tissue, are determined from  $N_{\text{cbms}}^{\text{abs}}$  curves by summation:

$$N_{\text{abs}} = \sum_{d=\text{min}}^{\text{max}} N_{\text{cbms}}^{\text{abs}}(d), \quad (20)$$

which is analogous to Equation 10. The final result is shown in Fig. 4(b), which is quite similar to Fig. 3(f). The only but very important difference between Fig. 3(e) and 3(f) on one side and Fig. 4 on the other side consists in the fact that the latter has vertical axis on absolute scale. Absolute numbers of wear par-

ticles given in Fig. 4(b) are around  $1 \times 10^{10}$ , which accords with the values found by other authors and methods [7, 18]. This also agrees with the following rough estimation: during every movement of loaded TJR about  $2 \times 10^5$  wear particles is produced [1], the number movements per year is estimated at  $1 \times 10^6$  [1]; multiplication of these two values equals  $2 \times 10^{11}$ . Considering that the particles come just from a few locations around TJR, the values in Fig. 4, which are approximately one order of magnitude lower than the estimate, look acceptable.

### 3.4. Verification of the results by means of other methods

In the last part of this study, the results from LS were verified using independent methods. The purpose was: (i) to prove that what we have observed with LS were UHMWPE particles and (ii) to check whether the sizes of the particles from LS are correct. Three samples were randomly selected from 72 samples measured with LS [13] and three methods (SEM, QELS and EDAX) were used to analyze each of the selected samples. SEM micrographs (Fig. 5) confirmed that the samples do contain both submicron particles and particles with several tens of micrometers in diameter as it had been observed in LS. QELS measurements confirmed that samples contain submicron particles but average QELS diameters of the particles are somewhat higher than average LS diameters of the particles (Table I). EDAX analysis proved that most of the particles are UHMWPE and confirmed that a small number of the particles might be bone fragments. Samples prepared for EDAX were UHMWPE particles on carbon blocks. According to EDAX analysis, most of the particles are UHMWPE because only carbon signals were detected

TABLE I Maxima on size distribution curves of UHMWPE wear particles as obtained by LS and QELS methods;  $d$  stands for equivalent diameter

Sample ID	$d$ [ $\mu\text{m}$ ] (LS)	$d$ [ $\mu\text{m}$ ] (QELS)
2/10	0.07	0.25
4/8	0.34	0.45
7/8	0.31	0.38

The samples are denoted as X/Y where X is the patient number and Y is the zone number.

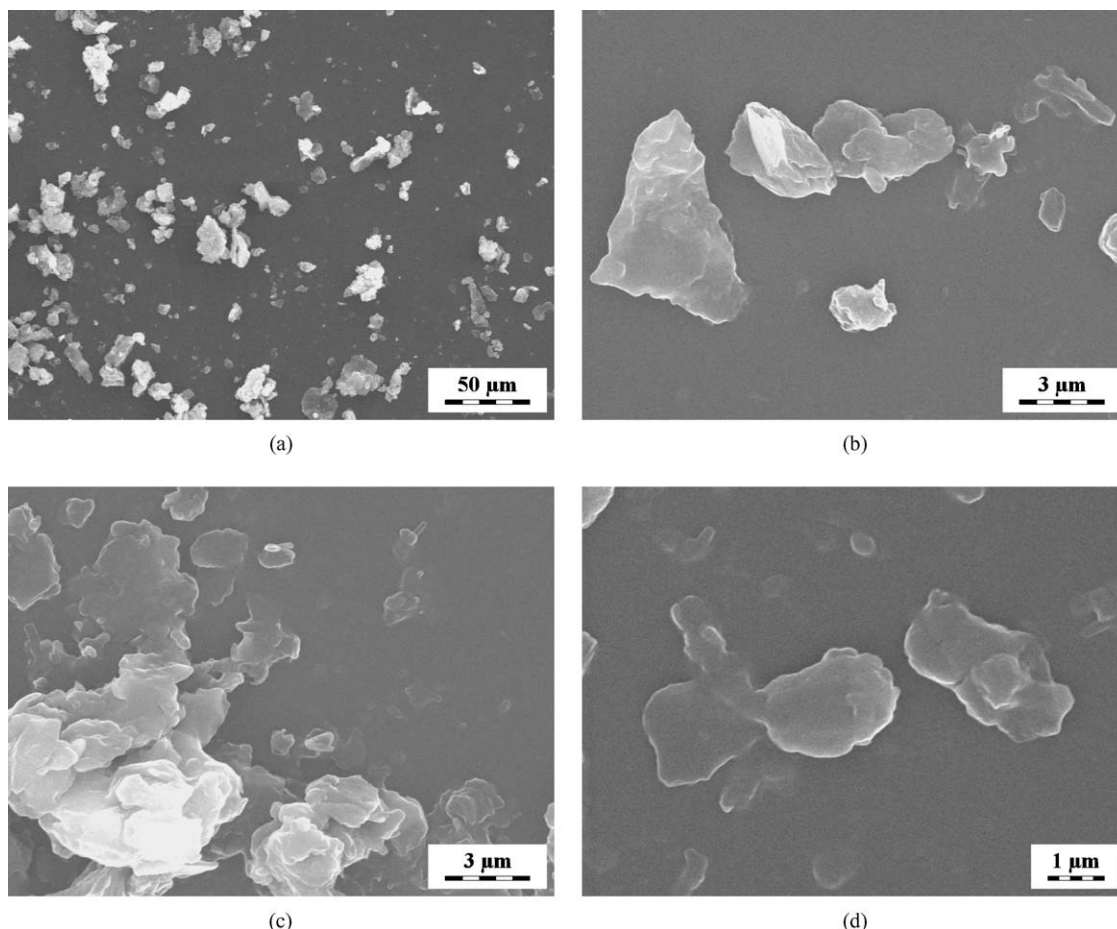


Figure 5 SEM micrographs of UHMWPE wear particles. The micrographs show particles that were obtained by evaporating a droplet of suspension of wear particles after isolation II (Chapter 2.2.2).

in most locations. The carbon signal came from both carbon blocks (pure graphite) and UHMWPE (carbon and hydrogen; hydrogen is undetectable with EDAX). However, on a few locations also other elements were found, above all Ca but also P, O and small amounts of Na, Cl and S. This accorded with our assumption that some samples contained a small amount of bone fragments, whose important part is hydroxylapatite,  $\text{Ca}_{10}(\text{PO}_4)_6(\text{OH})_2$  as had already been indicated by XRD and IR methods (Section 3.1). No N atoms were found, which proves that nitrates from isolation I were removed by dialysis (isolation II, Section 2.2.2).

#### 4. Discussion

The goal of this work was to develop an easy and fast method enabling the determination of the numbers of UHMWPE wear particles so that it was possible to study the distribution of wear particles around TJR's. The new method, called LSC, is based on LS and yields *relative* numbers of wear particles. It is worth noting that LSC needs just a simple isolation technique for wear particles (Section 2.2.1) and routine LS measurements (Section 2.6); all other methods were used here just to verify the results. A modification of the LSC method, called LSCm, requires *one* gravimetric analysis for all studied samples to yield *absolute* numbers of wear particles.

Several facts suggest that the results of LSC and LSCm methods yield correct results: (i) the LSC

method confirmed that most of the wear particles are below  $1 \mu\text{m}$ , which is in agreement with the literature [7–10, 17–19]. (ii) the LSC method confirmed the general and logical assumption that the distribution of the wear particles around TJR's is irregular. Moreover, the highest numbers of wear particles were frequently found at location 10 (Fig. 3). Samples from location 10 were available for 6 patients [13]. The highest number of wear particles at location 10 was found for 5 of the 6 patients. The last of the 6 patients had the highest numbers of wear particles at locations 7, 0 and 10. This common feature of the samples looks reasonable because location 10 is very close to the UHMWPE cup (Fig. 1). If the highest numbers of wear particles at location 10 are not random, which has to be confirmed by further studies, then this feature can be regarded as the confirmation of reproducibility and correctness of the method. (iii) the LSCm method yielded absolute numbers of wear particles that agree quite well with those found in the previous studies [7, 18]. It is worth noting that the precision of the LSCm method increases with increasing number of samples. The crucial step of the LSCm method is determination of constant  $x$  (Equations 13–15) from the experimentally determined mass of wear particles  $m_{\text{all}}^{\text{exp}}$  (Equation 13). The value of  $m_{\text{all}}^{\text{exp}}$  is determined by gravimetric analysis, whose weakest point is the very low mass of the wear particles. For example, in the work of McNie *et al.* [18] as low values as  $21 \mu\text{g}$  per one gram of wet acetabular

tissue were found in some samples. Such a low values can make the gravimetric analysis very imprecise. The LSCm method takes advantage of the fact that the *relative* amounts of wear particles are known *before* the gravimetric analysis and uses a mixture of all samples to determine *absolute* amounts of wear particles. The more samples are mixed, the higher is the value of  $m_{\text{all}}^{\text{exp}}$ , the lower is the relative error in gravimetric analysis and, as a result, the more precisely determined is the constant  $x$ , from which the absolute numbers of wear particles are determined. (iv) IR, SEM and EDAX analyses confirmed that the samples used for the LSC and LSCm methods do contain submicron particles and that those particles are mostly UHMWPE. (v) The overall shape of volume distribution curves (broad, gaussian-like peaks, mostly in the region with  $d > 10 \mu\text{m}$ ) and number distribution curves (sharp, asymmetric peaks, mostly in the region with  $d < 5 \mu\text{m}$ ) are quite similar to the shape of distribution curves from the work of Elfick *et al.* [26], who used LS to study the size of wear particles from joint simulators.

On the other hand, there are some facts indicating that the precision of the LSC and LSCm methods might be limited: (i) The maxima on number distribution curves obtained by the LSC method appear at lower  $d$  than the corresponding maxima from QELS distribution curves (Table I). This can be partially attributed to the intrinsic differences between the two methods because LS detects equivalent sphere diameters based on static light scattering whereas QELS detects hydrodynamically equivalent spheres. Anyway, the results for sample 2/10 (Table I), for patient 17 (Fig. 3(e)) and for several other patients [13], showing maximum number of particles with  $d$  cca  $0.07 \mu\text{m}$  seem too low. The maxima of number distributions obtained in previous studies are usually found at higher values of  $d$ , such as  $0.1\text{--}0.5 \mu\text{m}$  [9],  $0.1\text{--}0.5 \mu\text{m}$  [18],  $1.7 \mu\text{m}$  [19] and  $0.1\text{--}0.2 \mu\text{m}$  [28] although the recent study of Scott *et al.* [10] suggests that numbers of particles smaller than  $0.2 \mu\text{m}$  might have been underestimated in numerous studies. It seems as if the LS measurements reported smaller values of  $d$ , the error growing with decreasing size of the particle. The discrepancies might have been caused by small dimensions of the particles (Section 3.2, ref. [28]). The correct position of the maximum on number distribution curves requires application of a correct optical model (Section 2.6). Nevertheless, in this work several models were tested and the best results were obtained with the model identical to that from the analogous work of Elfick *et al.* [26]. (ii) The LSC method is based on the assumption that the addition of a known amount of calibration spheres introduces in the LS experiment quantitative information, which is precise enough to determine relative numbers of wear particles. It is also assumed that the relation between the LS peaks corresponding to wear particles and those corresponding to calibration spheres is linear, i.e. that the AuC (area under curve) increases linearly with increasing number of the particles relative to AuC corresponding to calibration spheres. These two assumptions were verified by a slightly modified LSC experiment, whose description follows. At first, a LS volume distribution

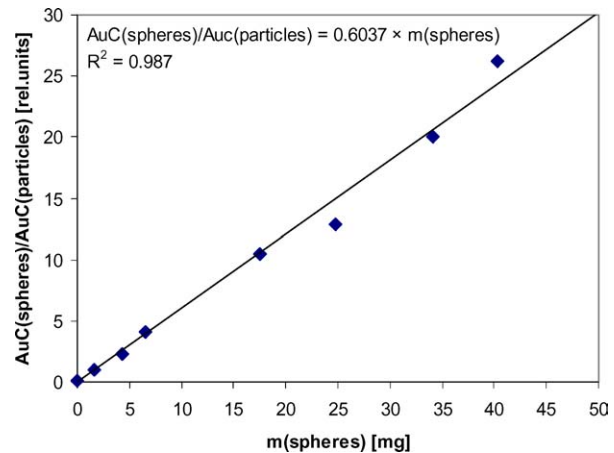


Figure 6 Check of linearity and precision of LSC method.

curve of a randomly selected suspension of wear particles was measured. At second, a known amount of calibration spheres ( $m_{\text{spheres}}$ ) was added to the suspension and the measurement was repeated. At third, another known amount of calibration spheres was added to the suspension etc. In the end,  $\text{AuC}_{\text{particles}}$  corresponding to wear particles ( $d = 0.04\text{--}300 \mu\text{m}$ ) and  $\text{AuC}_{\text{spheres}}$  corresponding to calibration spheres ( $d = 0.04\text{--}300 \mu\text{m}$ ) were determined and the ratio  $\text{AuC}_{\text{spheres}}/\text{AuC}_{\text{particles}}$  was plotted as a function of  $m_{\text{spheres}}$  (Fig. 6). The ratio  $\text{AuC}_{\text{spheres}}/\text{AuC}_{\text{particles}}$  increases linearly with the amount of calibration spheres, which means that it is possible to obtain information about relative number of some particles if we use another kind of particles as a reference. However, the average deviation of experimental values from the linear trend is as high as 5% and the highest deviation is as large as 14%. As both the LSC and LSCm methods are based on the ratios of peaks corresponding to wear particles and calibration spheres, it is possible to estimate that the average error of both absolute and relative numbers of wear particles is around 5% of the experimental value and the maximum error should be lower than 14% of the experimental value. (iii) LSC and LSCm methods are based on the validity of Equation 8. However, the equation is just an approximation as discussed in Section 3.2. The worse the approximation holds, the more the number distribution curves are distorted. For example, if  $\text{Const}$  in Equation 8 decreased with decreasing  $d$ , the numbers of smaller particles would be overestimated and the numbers of bigger particles would be overestimated. (iv) Several methods (IR, XRD, EDAX) indicated that there are bone fragments in some samples. However, it is reasonable to assume that the influence of the bone fragments on the results was not crucial as both IR and EDAX methods proved that the number of bone fragments was quite small. Moreover, a binodal distribution was observed in no sample, indicating that either the number of bone fragments is negligible or the bone fragments were of the same size as the wear particles in all samples, which is very unlikely.

The above considerations suggest that the LSC as LSCm methods have both advantages and disadvantages. The number distribution curves may be distorted

due to the limited validity of Equation 8. More precise distribution curves might be obtained by image analysis of electron micrographs [10] although light scattering techniques are preferred by some [26]. The numbers of wear particles may be imprecise as discussed in the previous paragraph. More precise numbers of particles might be obtained by gravimetric analyses on condition that sufficient amount of samples are available [7, 19]. However, easiness and quickness of LSC and LSCm methods is a great advantage if high numbers of samples have to be processed. If the main goal is a comparison of the samples, then the limited validity of Equation 8 does not matter so much provided that the samples are similar because possible inaccuracies are more-or-less the same for all samples. As for wear particles around TJR's, all samples are almost identical (Fig. 3, Section 3.2), which means that all the distribution curves of all samples are affected *in the same way* and so the *relative* values should be more-or-less correct and the comparison can be made. It is a matter of course that LSC and LSCm methods can be applied to any samples, which are suspensions containing particles scattering visible light. For example, application of LSC method to samples from joint simulators would save a great deal of experimental time because the LSC method, unlike popular weight loss method [12], does not require weighable amount of particles. The precision, usefulness and applicability of LSC and LSCm methods will emerge in the course of time. More information will appear in the near future [13].

## 5. Conclusion

The authors of this work tried to develop a new method for easy and fast determination of the numbers of UHMWPE wear particles. The new method, called LSC, is based on the light scattering of a suspension of wear particles *and* calibration spheres, and yields *relative* numbers of particles. A modified LSC method, called LSCm, requires *one* additional experiment, the gravimetric analysis of a mixture of all studied samples, to determine the *absolute* numbers of wear particles. The precision of the LSC and LSCm method may be somewhat lower but their easiness and quickness make them suitable for processing and comparing high numbers of samples.

## Acknowledgment

Financial support through grants No. S4050009 (Program for the support of task research and development of the Academy of Sciences of the Czech Republic), IGA MZ ČR 7076-3 (Internal Grant Agency of the Ministry of Health of the Czech Republic) and GACR 106/04/1118 (Grant Agency of the Czech Republic) is gratefully appreciated.

## References

1. H. A. KELLOP, P. CAMPBELL, S. H. PARK, T. P. SCHMALZRIED, P. GRIGORIS, H. C. AMSTUTZ and A. SARMIENTO, *Clin. Orthop.* **311** (1995) 3.

2. M. A. WIRTH, C. M. AGRAWAL, J. D. MABREY, D. D. DEAN, C. R. BLANCHARD and M. A. MILLER, *J. Bone Joint Surg. Am.* **81** (1999) 29.
3. J. D. MABREY, A. AFSAL-KESHMIRI, G. A. ENGH, C. J. SYCHTERZ, M. A. WIRTH, C. A. ROCHWOOD and C. M. AGRAWAL, *J. Biomed. Mater. Res.* **63** (2002) 475.
4. T. R. GREEN, J. FISHER, J. B. MATTHEWS, M. H. STONE and E. INGHAM, *ibid.* **53** (2000) 490.
5. M. M. ENDO, P. S. M. BARBOUR, D. C. BARTON, J. FISHER, J. L. TIPPER, E. INGHAM and M. H. STONE, *Bio-Med. Mater. Eng.* **11** (2001) 23 and references therein.
6. A. SOSNA, T. RADONSKÝ, D. POKORNÝ, D. VEIGL, Z. HORÁK and D. JAHODA, *Acta Chir. Orthop. Traumatol. Cech.* **1** (2003) 6.
7. K. J. MARGEVICIUS, T. W. BAUER, J. T. MCMAHON, S. A. BROWN and K. MERRITT, *J. Bone Joint Surg. Am.* **76A** (1994) 1664.
8. W. J. MALONEY, R. L. SMITH, T. P. SCHMELZRIED, J. CHIBA, D. HUENE and H. RUBASH, *ibid.* **77** (1995) 1301.
9. J. L. TIPPER, E. INGHAM, J. L. HAILEY, A. A. BESONG and J. FISHER, *J. Mater. Sci.—Mater. Med.* **11** (2000) 117.
10. M. SCOTT, K. WIDDING and S. JANI, *Wear* **250** (2001) 1213.
11. J. LIVERMORE, D. ILSTRUP and B. MORREY, *J. Bone Joint Surg. Am.* **72** (1990) 518.
12. S. NIEDZWIECKI, C. KLAPPERICH, J. SHORT, S. JANI, M. RIES and L. PRUITT, *J. Biomed. Mater. Res.* **56** (2001) 245.
13. A. SOSNA, D. POKORNÝ, T. RADONSKÝ, G. ENTLICHER and M. ŠLOUF, Z. HORÁK, in preparation.
14. R. DICKERFOFF and A. VONRUECKER, *Clin. Lab. Haematol.* **17** (1995) 163.
15. A. P. D. ELFICK, S. M. GREEN, S. KRICKLER and A. UNSWORTH, *J. Biomed. Mater. Res. A* **65A** (2003) 95.
16. T. A. GRUEN, G. M. MCNEICE and H. C. AMSTUTZ, *Clin. Orthop.* **141** (1979) 17.
17. J. G. DELEE and J. CHARNLEY, *Clin. Orthop.* **121** (1976) 20.
18. C. M. MCNIE, D. C. BARTON, E. INGHAM, J. L. TIPPER and J. FISHER, *J. Mater. Sci. — Mater. M.* **11** (2000) 163.
19. A. S. SHANBHAG, H. O. BAILEY, D. HWANG, C. V. CHA, N. G. EROR and H. E. RUBASH, *J. Biomed. Mater. Res.* **53** (2000) 100.
20. B. P. SAVILLE, in "Applied Polymer Light Microscopy" edited by D. A. Hemsley (Elsevier, London, 1989) p. 111.
21. H. C. HULST, in "Light Scattering by Small Particles" (John Wiley & Sons, New York, 1957) p. 23.
22. *Idem.*, in "Light Scattering by Small Particles" (John Wiley & Sons, New York, 1957) p. 8.
23. Coulter LS Series Product Manual. USA, Miami, Coulter Corporation, 1994. p. 14.
24. K. YVON, W. JEITSCHKO and E. PARTHĚ, *J. Appl. Cryst.* **10** (1977) 73.
25. Inorganic Crystal Structure Database. Germany, Fachinformationzentrum Karlsruhe, 2000.
26. A. P. D. ELFICK, S. L. SMITH, S. M. GREEN and A. UNSWORTH, *Wear* **249** (2001) 517.
27. H. C. HULST, in "Light Scattering by Small Particles" (John Wiley & Sons, New York, 1957) p. 385.
28. A. WANG, A. ESSNER, C. STARK and J. H. DUMBLETON, *Biomaterials* **17** (1996) 865.

Received 23 October 2003  
and accepted 23 June 2004